arXiv:1409.1424v1 [astro-ph.SR] 4 Sep 2014

Radio timing and optical photometry of the black widow system PSR J1518+0204C in the globular cluster M5[1]

C. Pallanca[1], S. M. Ransom[2], F. R. Ferraro[1], E. Dalessandro[1], B. Lanzoni[1], J. W. T. Hessels[3,4], I. Stairs[5], P. C. C. Freire[6]

[1] *Dipartimento di Fisica e Astronomia, Università di Bologna, Viale Berti Pichat 6/2, I-40127 Bologna, Italy*

[2] *National Radio Astronomy Observatory (NRAO), 520 Edgemont Road, Charlottesville, Virginia 22901, USA.*

[3] *ASTRON, the Netherlands Institute for Radio Astronomy, Postbus 2, 7990 AA, Dwingeloo, The Netherlands*

[4] *Anton Pannekoek Institute for Astronomy, University of Amsterdam, Science Park 904, 1098 XH Amsterdam, The Netherlands*

[5] *Department of Physics and Astronomy, University of British Columbia, 6224 Agricultural Road Vancouver, BC V6T1Z1, Canada*

[6] *Max-Planck-Institute für Radioastronomie, D-53121 Bonn, Germany*

04 September, 2014

ABSTRACT

We report on the determination of astrometric, spin and orbital parameters for PSR J1518+0204C, a "black widow" binary millisecond pulsar in the globular cluster M5. The accurate position and orbital parameters obtained from radio timing allowed us to search for the optical companion. By using WFC3/HST images we identified a very faint variable star ($m_{F390W} \gtrsim 24.8$, $m_{F606W} \gtrsim 24.3$, $m_{F814W} \gtrsim 23.1$) located at only $0.25''$ from the pulsar's timing position. Due to its strong variability, this star is visible only in a sub-sample of images. However, the light curve obtained folding the available data with the orbital parameters of the pulsar shows a maximum at the pulsar inferior conjunction and a possible minimum at the pulsar superior conjunction. Furthermore, the shape of the optical modulation indicates a heating process possibly due to the pulsar wind. This is the first identification of an optical companion to a black widow pulsar in the dense stellar environment of a globular cluster.

Subject headings: Pulsars: Individual: PSR J1518+0204C, Globular clusters: Individual: M5 (NGC 5904), Techniques: photometric

1. INTRODUCTION

According to the canonical formation scenario, millisecond pulsars (MSPs) form in binary systems containing a neutron star (NS) eventually spun up to millisecond periods by mass accretion from an evolving companion, that, in turn, is expected to become a white dwarf (WD; e.g Lyne et al. 1987; Alpar et al. 1982; Bhattacharya & van den Heuvel 1991). About 40% of known MSPs are found in globular clusters[2] (GCs), although the Galaxy is 100 times more massive ($2.4 \times 10^{11} \leq M/M_{\odot} \leq 1.2 \times 10^{12}$; Little & Tremaine 1987; Kochanek 1996) than the entire GC system. This is partially caused by selection effects, since GCs have been searched very deeply by radio surveys. Despite this, the over-abundance of MSPs in GCs compared to the Galactic disk is real and very large, and provides a strong indication that dynamical interactions greatly enhance the formation of these objects. In fact, in the Galactic field the only viable formation channel for MSPs is the evolution of primordial binaries, while in GCs dynamical interactions can promote the formation of binaries suitable for recycling NSs into MSPs (e.g., Davies & Hansen 1998). In particular, the ultra-dense cores of GCs are very efficient "factories" for generating exotic objects, such as low-mass X-ray binaries, cataclysmic variables, blue stragglers and MSPs (e.g. Bailyn 1995; Verbunt et al. 1997; Ferraro et al. 2001a). Indeed, these objects are thought to result from the evolution of various kinds of binary systems originated and/or hardened by stellar interactions (e.g. Clark 1975; Hills & Day 1976; Bailyn 1992; Ivanova et al. 2008), and are therefore considered as powerful diagnostics of GC dynamical evolution (e.g. Ferraro et al. 1995; Goodman & Hut 1989; Hut et al. 1992; Meylan & Heggie 1997; Pooley et al. 2003; Fregeau 2008; Ferraro et al. 2009, 2012).

Studying the optical emission properties of binary MSP companions is important to better constrain the orbital parameters and to clarify the evolutionary status of these systems. In GCs, it also represents a crucial tool for quantifying the occurrence of dynamical interactions,

---

[1]Based on observations collected with the NASA/ESA HST (Prop. 19835), obtained at the Space Telescope Science Institute, which is operated by AURA, Inc., under NASA contract NAS5-26555.

[2]see *http://www.naic.edu/∼pfreire/GCpsr.html* for an updated list

understanding the effects of crowded stellar environments on the evolution of binaries, determining the shape of the GC potential well, and estimating the mass-to-light ratio in the GC cores (e.g., Phinney 1992; Bellazzini et al. 1995; Possenti et al. 2003; Ferraro et al. 2003a). Despite their importance, only eight MSP companions in six GCs have been identified so far (Edmonds et al. 2001; Ferraro et al. 2001a; Edmonds et al. 2002; Sigurdsson et al. 2003; Ferraro et al. 2003b; Bassa et al. 2003; Cocozza et al. 2008; Pallanca et al. 2010, 2013b). Three of them are likely helium WDs, in agreement with the expectations of the MSP recycling scenario, while the other five are non-degenerate stars, which are thought to be either the result of a different evolutionary path or the product of an exchange interaction.

"Black Widows" (BWs) are MSPs characterized by an unmeasurably small eccentricity and a very small mass function (thus indicating a companion mass smaller than $0.05 M_{\odot}$; Roberts 2013). In most cases these pulsars show eclipses in the radio signal suggesting that the companion is a non-degenerate, possibly bloated star. In particular, in some systems the radio eclipse lasts for a significant fraction of the orbit, implying that the eclipsing region at the position of the companion is larger than its Roche lobe (RL). This suggests that the obscuring material is the plasma released by the companion because of the energy injected by the pulsar.

After the discovery of the first BWs in GCs, King et al. (2003) observed that they represented a much larger fraction of the MSP population than in the Galactic disk. Because of this, they proposed that BWs form much more often than other types of MSPs in GCs, going even as far as to suggest that perhaps they form *exclusively* in GCs and that the BWs in the Galactic disk were formed in GCs and later ejected. However, in the last years the number of BWs discovered in the Galactic field has significantly increased, both in blind surveys (Burgay et al. 2006; Bates et al. 2011; Keith et al. 2012) and particularly in the surveys targeted at Fermi unidentified sources (e.g., Ransom et al. 2011; Keith et al. 2011) suggesting that BWs can form directly in binary systems in the Galactic field, with no need for an exchange interaction. If this view is correct, then the percentages of BWs as a fraction of the total MSP population should be similar in the Galaxy and in GCs, particularly the GCs with a low interaction rate *per binary* Verbunt & Freire (2014): In both environments, an LMXB, once formed, can evolve undisturbed towards the MSP binary stage. Some BWs should survive even in GCs with a high interaction rate per binary, because they have very small orbits that are unlikely to be disrupted. Hence studying the numbers and properties of BWs both in the Galactic field and in GCs is important to test these two hypotheses (formation through dynamical interactions or the evolution of primordial binaries). This is important because their formation is still very poorly understood.

Up to now, only a few companions to BWs have been detected (Fruchter et al. 1988;

Stappers et al. 1996b, 1999, 2000; Reynolds et al. 2007; van Kerkwijk et al. 2011; Pallanca et al. 2012; Romani 2012; Breton et al. 2013), none of them in a GC. The companions to BWs in the Galactic field are found to be low-mass objects likely ablated and with a partially filled RL. Moreover, these objects show an IR/optical/UV modulation of a few magnitudes correlated with the orbital motion. The light curve of BW companions is usually characterized by a maximum around pulsar inferior conjunction ($\Phi \sim 0.75$) and one minimum around pulsar superior conjunction ($\Phi \sim 0.25$). This shape is thought to be due to the pulsar wind heating the side of the companion that faces the pulsar.

Here we present the first identification of an optical companion to a BW pulsar in the GC M5. M5 (NGC 5904) is a dynamically evolved GC (Ferraro et al. 2012) with intermediate central density and concentration ($\log \rho_0 = 4.0$ in units of $M_\odot/\mathrm{pc}^3$; Pryor & Meylan 1993; c=1.66; Miocchi et al. 2013) and relatively high metallicity ([Fe/H] $\sim$ -1.3, Carretta et al. 2009) located at ~ 7.5 kpc from the Earth (Ferraro et al. 1999; Harris 1996, 2010 version). M5 harbors five MSPs (Anderson et al. 1997; Hessels et al. 2007; Freire et al. 2008). Among them, PSR J1518+0204C deserves special attention since it is a BW system. This pulsar has a spin period of 2.48 ms and it is in a 2.1-hr orbit with a companion of minimum mass $\sim 0.04 M_\odot$. It shows regular eclipses for 15% of its orbit, as well as eclipse delays at eclipse ingress and egress, which can last up to 0.2 ms, and are presumably due to dispersive delays as the pulsar passes through the ionized wind of its companion (Hessels et al. 2007). If BWs are directly created in binary systems without the need for exchange interactions, then PSR J1518+0204C should resemble the BWs in the Galactic field. In fact, the very short orbital period ($\sim$ 2 hr) and M5's very low interaction rate per binary both suggest that it unlikely that PSR J1518+0204C was significantly disturbed following the LMXB stage.

In Sect. 2 the results of the radio timing are reported, while the optical observations and the identification of the companion to the pulsar are described in Sect. 3. The results are discussed in Sect. 4. In Sect. 5 we present some concluding remarks with attention to possible future studies.

2. RADIO TIMING

2.1. Observations and data processing

PSR J1518+0204C was discovered as part of a series of deep 1.4-GHz observations of several GCs with the Arecibo telescope in the summers of 2001 and 2002. Details of the search observations, methodology, and follow-up timing measurements of the new pulsars are described in detail by Hessels et al. (2007), and so we only briefly discuss the timing

observations and methodology for PSR J1518+0204C here.

All observations were made using one to four Wideband Arecibo Pulsar Processors (WAPPs; Dowd et al. 2000), each of which provides 100 MHz of bandwidth. We took observations in search mode, resulting in data with 256 frequency channels per WAPP, and a time resolution of 64 μs. In order to avoid known sources of radio frequency interference (aka RFI), one WAPP was centered near 1170 MHz and the remaining 2−3 WAPPs were placed such that together they covered a continuous frequency band of 200 or 300 MHz centered near 1470 MHz.

In the early years (2002-2004), we were taking many observations scattered through the year in order to better determine the astrometric and spin parameters for all the pulsars in the cluster. Since then, we have prioritized 1-week campaigns in order to improve the measurement of the rate of advance of periastron of M5B, as detailed in Freire et al. (2008), with a few scattered observations that helped improve the proper motions of all the pulsars. Given the short orbital period of M5C, we get excellent, but quasi-random orbital coverage of this pulsar, since the observing strategy has been mostly designed with M5B in mind.

The data were processed using standard techniques (e.g. Lorimer & Kramer 2012) with tools in the `PRESTO`[3] software suite. We folded the lower and contiguous upper frequency bands modulo the predicted pulse period using `prepfold`, removed strong narrow-band or transient broad-band RFI as identified by eye from the folds, then averaged the high signal-to-noise detections together to make a template pulse profile. We determined times of arrival (TOAs) every 3−15 minutes (based on the strength of the detection, primarily due to diffractive scintillation) by cross-correlating the template profile with the folded data using the routine `get_TOAs.py`[4], resulting in 2078 TOAs covering a period of about 9 years.

We determined a phase-connected timing solution using `TEMPO`[5], by fitting for astrometric, spin, and orbital parameters, along with a single average dispersion measure. We corrected arrival times to the TT(BIPM) time standard and used the DE421 solar system ephemerides (Folkner et al. 2008). Only 1398 TOAs were actually used in the fit as we ignored those TOAs between orbital phases of 0.2−0.38 due to the regular pulsar eclipse and the pulse delays during eclipse egress which would systematically skew orbital parameter fits. The eccentricity of the 2.08-hr orbit was too small to measure and we therefore fixed it, as well as the argument of periapsis (ω), both to zero.

---

[3] `http://www.cv.nrao.edu/~sransom/presto`

[4] The `get_TOAs.py` routine is based on the algorithm described by Taylor (1992).

[5] `http://tempo.sourceforge.net`

The final timing solution, reported in Table 1 and shown in Figure 1, had weighted RMS residuals of 12.3 μs and a reduced-χ^2 of 1.88 with 1385 degrees-of-freedom. We estimated the errors on the fit parameters using a bootstrap error analysis with 4096 iterations.

2.2. Results

The timing solution includes a very precise position and proper motion, which are absolutely required for follow-up of the object in the crowded field of M5. The system is located at α(J2000) = $15^{\rm h}18^{\rm m}32\overset{\rm s}{.}788893(21)$ and δ(J2000) = $02^\circ04'47\overset{''}{.}8153(8)$, which is only 7.5″ (corresponding to ~ 0.27 core radii; $r_c = 28''$) from the nominal cluster center as determined by Miocchi et al. (2013). This is well within the core radius of the cluster. The proper motion is entirely consistent with the previously measured proper motions of PSR B1516+02A and B (Freire et al. 2008), indicating that it is mostly due to the motion of the cluster as a whole. The peculiar velocities of these pulsars within the cluster are still too small to be measured with our current timing precision.

The observed spin period derivative of the pulsar is a combination of several contributions, the main ones being due to its intrinsic spin period derivative, $\dot{P}_{\rm int}$, the acceleration of the pulsar in the gravitational field of the cluster projected along the line of sight a_l and the Shklovskii's effect, due to the pulsar's total proper motion μ:

$$\left(\frac{\dot{P}}{P}\right)_{\rm obs} = \left(\frac{\dot{P}}{P}\right)_{\rm int} + \frac{a_l}{c} + \frac{\mu^2 d}{c}, \tag{1}$$

where d is the distance to the cluster, 7.5 kpc. The Galactic acceleration is generally small or of the same order as the last term, which is the smallest.

Using a simple empirical model of GC interiors (King 1962; Freire et al. 2005) and the cluster's central velocity dispersion of 5.5 km s^{-1} (Harris 1996, 2010 version), we estimate that the maximum cluster acceleration along the line of sight at the location of M5C is $a_{\rm max} = \pm 1.54 \times 10^{-9}{\rm ms}^{-2}$. This would need to be of the order of $\pm 2.6 \times 10^{-9}{\rm ms}^{-2}$ to fully account for the observed $\dot{P}$ already without the contribution from the Shklovskii effect (which amounts to $+0.5 \times 10^{-9}{\rm ms}^{-2}$). From this, we can infer minimum and maximum values for $\dot{P}_{\rm int}$ of 0.9 and 3.5×10^{-20}, which implies a magnetic field $1.5\times < B_0 < 3.0 \times 10^8$ G and a characteristic age $1.1 < \tau_c < 4.3$ Gyr. These values are typical among the Galactic MSP population.

We also detect a variation of orbital period with very high significance; its time derivative $\dot{P}_{orb}$ is $-0.914(23) \times 10^{-12}$. Considering the typical masses of such binary systems the

measured value is one order of magnitude larger than the expected contribution due to the emission of gravitational waves predicted by general relativity. Such a discrepancy is a common feature for BW systems (Lazaridis et al. 2011), where significant changes of the orbit are most likely caused by tidal dissipation leading to changes in the gravitational quadrupole moment of the companion (which are not negligible in the case of a distorted companion, or in the presence of an interaction between the companion and the pulsar; Lorimer et al. 2004, and references therein). The effect is *not* due to the acceleration of the pulsar in the cluster: even if it were accelerating with $\pm a_{\rm max}$, the contribution to the orbital variation would only be $\dot{P}_{orb,k} = \pm 0.04 \times 10^{-12}$.

We also detect a variation of the apparent slowdown of the pulsar, $\ddot{\nu}$, although with much lower significance. This is likely caused by a small change in the gravitational acceleration of the cluster and nearby stars at the position of the pulsar, something to be expected considering that the pulsar is, at least in projection, very near the center of the cluster, where the stellar density is highest.

3. OPTICAL PHOTOMETRY OF THE COMPANION STAR

3.1. Observations and data analysis

By taking advantage of the precise position of PSR J1518+0204C obtained from the radio timing, we used high resolution Hubble space telescope (HST) images to search for the optical companion to this pulsar. The photometric data-set consists of a set of images obtained with the ultraviolet-visible (UVIS) channel of the WFC3. The WFC3 UVIS CCD consists of two twin detectors with a pixel-scale of $\sim 0.04''$/pixel and a global field of view (FOV) of $\sim 162'' \times 162''$. Our analysis has been focused only on CHIP1, which contains the pulsar region.

The analyzed images have been acquired through four filters, in two different epochs. The first epoch images have been obtained on 2010 July 5 (Prop. 11615, P.I. Ferraro). The data-set consists of: 6 images in the F390W filter with an exposure time $t_{\rm exp} = 500$ s each, 4 images in F606W with $t_{\rm exp} = 150$ s, 4 images in F814W with $t_{\rm exp} = 150$ s, and 6 images in F656N (a narrow filter corresponding to Hα) with exposure times ranging from $t_{\rm exp} = 800$ s to $t_{\rm exp} = 1100$ s. The second epoch images have been obtained during four visits between 2012 June 6 and 2012 June 9 (Prop. 12517, P.I. Ferraro), using the same three wide filters as the first epoch. In particular, the data-set consists of: 4 images obtained through the F390W filter with an exposure time $t_{\rm exp} = 735$ s each, 8 images in F606W with $t_{\rm exp} = 350$ s, and 12 images in F814W with $t_{\rm exp} = 230$ s and 240 s.

The photometric analysis has been performed on the WFC3 "flat fielded" (flt) images, once corrected[6] for "Pixel-Area-Map" (PAM) by using standard IRAF procedures. The photometric analysis has been carried out by using the DAOPHOT package (Stetson 1987). For each image we modeled the point spread function (PSF) by using a large number (~ 100) of bright and nearly isolated stars. The PSF model and its parameters have been chosen by using the DAOPHOT `PSF` routine on the basis of a Chi-squared test. A Moffat function (Moffat 1969) provides the best fit to the data in all cases. All F390W, F606W and F814W images have been combined with DAOPHOT `MONTAGE2` in order to produce a master frame. On this combined image we then performed a source detection analysis by using DAOPHOT `FIND` and a 3σ detection limit, where σ is the standard deviation of the measured background. Finally, using the star list thus obtained as a reference master list, we performed the PSF-fitting in each image by using the DAOPHOT packages `ALLSTAR` and `ALLFRAME` (Stetson 1987, 1994). For each star the magnitudes estimated in different images have been homogenized (see Ferraro et al. 1991, 1992) and their weighted mean and standard deviation have been finally adopted as the star mean magnitude and its photometric error. In the final catalog we reported both single image magnitudes and the mean magnitudes in each filter.

Since the FOV of the WFC3 images suffers heavily from geometric distortions, we corrected the instrumental positions of stars by applying the equations reported by Bellini & Bedin (2009) and Bellini et al. (2011). We then transformed the WFC3 catalog to the absolute astrometric system (α, δ) by using the stars in common with the HST WFPC2 catalog from Lanzoni et al. (2007) as secondary astrometric standards, by using the cross-correlation software CataXcorr[7]. The astrometric solution has an accuracy of $\sim 0.2''$ in both α and δ.

Finally, the WFC3 instrumental magnitudes have been calibrated to the VEGAMAG system by using the photometric zero-points and the procedures reported on the WFC3 web page.[8]

---

[6]For more details on the applied correction and on the Pixel Area Map definition see the WFC3 Data Handbook.

[7]CataXcorr is a code aimed at cross-correlating catalogs and finding astrometric solutions, developed by P. Montegriffo at INAF - Osservatorio Astronomico di Bologna. This package, available at *http://davide2.bo.astro.it/∼paolo/Main/CataPack.html*, has been successfully used in a large number of papers by our group in the past 10 years.

[8]http://www.stsci.edu/hst/wfc3/phot_zp_lbn

3.2. The companion to PSR J1518+0204C

In order to identify the companion to PSR J1518+0204C we searched for peculiar objects located within 1″ from the nominal pulsar position (see Table 1). At a first visual inspection of the pulsar region, it was possible to identify a star showing strong variability and lying at $\sim 0.25''$ from the pulsar, which is within the optical astrometric uncertainty. This star is very faint and visible only in a few images, while it is below the detection limit in the other frames (see Figure 2).

For this reason we performed a visual inspection of all the 44 available images, whenever possible forcing the fitting procedure to determine the magnitude of this faint star. We were able to measure its magnitude in only 14 images (4 in the F390W, 3 in the F606W and 7 in the F814W filters) however this limited data set was sufficient to clearly assess the variability of this star, which showed quite significant luminosity variations: $\Delta m_{F390W} \sim 0.32$ mag (from $m_{F390W} = 24.83 \pm 0.17$ to $m_{F390W} = 25.15 \pm 0.22$), $\Delta m_{F606W} \sim 0.62$ mag (from $m_{F606W} = 24.34 \pm 0.20$ to $m_{F606W} = 24.96 \pm 0.19$), and $\Delta m_{F814W} \sim 0.87$ mag (from $m_{F814W} = 23.13 \pm 0.07$ to $m_{F814W} = 24.00 \pm 0.28$). Unfortunately, the object is under the detection threshold in all F656N images, hence we do not have any m_{F656N} measure. In the other images this star is not detected, most likely because its flux is below the detection threshold. For each band, we estimated the detection threshold as the average value of the magnitudes of the five faintest detected stars within 20″ from the pulsar position, obtaining $DT_{F390W} \sim 26.59 \pm 0.13$, $DT_{F606W} \sim 25.67 \pm 0.10$ and $DT_{F814W} \sim 24.41 \pm 0.14$. In turn, these values imply the following lower limits to the amplitudes of variation: $\Delta m_{F390W} \geq 1.76$, $\Delta m_{F606W} \geq 1.33$ and $\Delta m_{F390W} \geq 1.28$. Moreover this star shows a magnitude scatter larger than that computed for objects of similar luminosity.

In order to establish whether the magnitude of variation is related to the pulsar's orbital phase (and hence establish a physical connection between this star and the pulsar), we computed the light curve in the three bands folding each measurement (using a magnitude upper limit for the images where the star is not detected) with the orbital period and the ascending node of the pulsar (see Table 1). Although the available data do not allow a complete coverage of the orbital period, the flux modulation of the star nicely correlates with the pulsar's orbital phase (see Figure 3). In fact, the data are consistent with a luminosity maximum (in each band) around $\Phi = 0.75$, corresponding to the pulsar inferior conjunction (when we are observing the companion side facing the pulsar) and a luminosity minimum (at least a few magnitudes fainter) around $\Phi = 0.25$, corresponding to the pulsar superior conjunction (when we are observing the back side of the companion). Such a shape is the typical light curve expected when the surface of the companion is heated by the pulsar flux.

For reference, we over-plotted sinusoidal functions[9] with a maximum at $\Phi = 0.75$ and a minimum at $\Phi = 0.25$ onto the observed light curve. The first important point to note is that in order to account for most of the upper limits where the star is not detected, an amplitude variation of about three magnitudes is required (see Figure 3). Such a large modulation (Δmag$\sim$ 3 mags) is in good agreement with what is observed for similar objects in the Galactic field (e.g. Stappers et al. 1999, 2001; Pallanca et al. 2012). Second, despite the low significance of the detection, there are some hints that the light curve could be asymmetric (e.g. the decrease to minimum seems to be steeper than the increase to maximum), possibly due to an asynchronously rotating companion as in the case of PSR J2051−0827 (Doroshenko et al. 2001; Stappers et al. 2001).

As evident from Figure 2 two other stars are located within the optical astrometric uncertainties. In the color magnitude diagrams (CMDs) they are both located in the lowest part of the main sequence and from a variability analysis their light curves appear to be dominated by the large photometric errors. In particular they seem to have different behaviors in the various filters and they do not show any correlation with the orbital motion of the system. Hence, we can safely rule out these objects as possible candidate companions.

All these pieces of evidence suggest that the identified variable star is the companion to PSR J1518+0204C and we name it COM-M5C. Since the available m_{F390W}, m_{F606W} and m_{F814W} measurements do not allow us to have reliable measures of the mean magnitudes of this star, in the following analysis we will use the values at maxima ($m_{F390W} = 24.83$, $m_{F606W} = 24.34$ and $m_{F814W} = 23.13$) and a plausible range of magnitude variation ($\sim$ 3 mags).

Figure 4 shows the position of COM-M5C in the (m_{F606W}, $m_{F606W} - m_{F814W}$) and in the (m_{F390W}, $m_{F390W} - m_{F606W}$) CMDs. As can be seen, COM-M5C is located at faint magnitudes between the main sequence (MS) and the WD cooling sequence, thus suggesting that it is probably a non-degenerate or a semi-degenerate, low mass, swollen star. Indeed similar objects have been previously identified in Galactic GCs (see Ferraro et al. 2001b; Edmonds et al. 2002; Cocozza et al. 2008; Pallanca et al. 2010, 2013b).

[9]Note that the light curve can be more complicated than a sinusoid, as found for a few Galactic field BWs by Breton et al. (2013).

4. DISCUSSION

We have constrained the mass, luminosity and temperature of COM-M5C by comparing its position in the (m_{F606W}, $m_{F606W} - m_{F814W}$) CMD (Figure 4) with a reference isochrone well reproducing the main evolutionary sequences of MS stars (Girardi et al. 2000; Marigo et al. 2008). We adopted a metallicity [Fe/H] $\sim$ -1.3 (Carretta et al. 2009), an age t = 13 Gyr, a distance modulus $(m - M)_0$=14.37 and a color excess $E(B - V) = 0.03$ (Ferraro et al. 1999). In particular, for the magnitude of the companion we assumed the value at maximum ($m_{F606W} = 24.34$) as an upper limit to the luminosity and for its color we adopted the value at maximum ($m_{F606W} - m_{F814W} = 1.21 \pm 0.46$) as a reference. The color uncertainty has been estimated from the typical photometric error of stars of similar magnitudes (see the gray shaded region in Figure 4). The resulting effective temperature, luminosity and mass of the companion are 3440K $\lesssim T_{\rm eff} \lesssim$ 5250K, $L \lesssim 1.19 \times 10^{-2} L_{\odot}$ and $M_{\rm COM} \lesssim 0.2 M_{\odot}$. Given that both the luminosity and temperature of the companion are overestimated, the comparison with the adopted theoretical isochrone gives an upper limit to the companion mass.

Note that if we consider the largest derived value of the mass ($M_{\rm COM} \sim 0.2 M_{\odot}$) and we combine it with the pulsar mass function, we can rule out very small inclination angles (e.g., $i \lesssim 10^{\circ}$ for a $1.4 M_{\odot}$ NS). However, as found for other companion stars (e.g. Ferraro et al. 2003c; Pallanca et al. 2010; Mucciarelli et al. 2013), masses of perturbed stars derived from their position in the CMD might be overestimated[10]. On the other hand, if we assume the lower mass limit for core hydrogen burning stars ($M_{\rm COM} = 0.08 M_{\odot}$) we would obtain an upper limit to the inclination angle of the system $i < 30^{\circ}$. However, such inclinations would be in disagreement with the presence of a radio eclipse.

Under the assumption that the optical emission of COM-M5C is well reproduced by a blackbody (BB), the stellar radius is $R_{\rm BB} \lesssim 0.30\ R_{\odot}$. However, companions to BWs are expected to be affected by the tidal distortion exerted by the pulsar and consequently to be swollen up to fill their RL. Hence, to justify the presence of eclipses of the radio signal, the size of the RL might be a more appropriate value (e.g., see PSR J2051−0827 and PSR J0610−2100 Stappers et al. 1996b, 2000; Pallanca et al. 2012). According to Eggleton (1983) the RL radius can be computed as:

$$\frac{R_{\rm RL}}{a} \simeq \frac{0.49 q^{\frac{2}{3}}}{0.6 q^{\frac{2}{3}} + \ln\left(1 + q^{\frac{1}{3}}\right)}$$

[10] In fact, from the measured luminosity we can directly derive the mass through comparison with models of unperturbed MS stars, but if the star filled the RL (and thus no longer follows the hydrostatic equilibrium law) such a mass value could be overestimated.

where q is the ratio between the companion and the pulsar masses ($M_{\rm COM}$ and $M_{\rm PSR}$, respectively) and a is the orbital separation. This relation can be combined with the pulsar mass function $f_{\rm PSR}(i, M_{\rm PSR}, M_{\rm COM}) = (M_{\rm COM} \sin i)^3/(M_{\rm COM} + M_{\rm PSR})^2$. By assuming a NS mass ranging from $\sim 1.2 M_\odot$ to $2.5 M_\odot$ (Özel et al. 2012) and leaving the inclination angle to span the entire range of values (between 1° and 90°), this yields $R_{\rm RL} \sim 0.13 - 0.89\ R_\odot$.

Under the assumption that the optical variation shown in Figure 3 is mainly due to irradiation from the MSP, reprocessed by the surface of COM-M5C, we can estimate how the re-processing efficiency depends on the inclination angle and, hence, infer the companion mass. To this end, one can compare the observed flux variation (ΔF_{obs}) between the maximum ($\Phi = 0.75$) and the minimum ($\Phi = 0.25$) of the light curve, with the expected flux variation (ΔF_{exp}) computed from the rotational energy loss rate ($\dot{E}$). Unfortunately, $\dot{E}$ is not measurable with the available radio observations, because the observed period derivative is likely significantly affected by acceleration of the pulsar in the gravitational potential of the cluster. However we took as reference the value measured for some BWs in the Galactic field, which typically have $\dot{E}$ values ranging from 10^{34} to 10^{35} erg s^{-1} (Breton et al. 2013). Actually, since we do not observe the entire light curve, ΔF_{obs} can just put a lower limit to the reprocessing efficiency.

At first we converted the observed $\Delta {\rm m}_{\rm F606W}$ modulation into a flux variation. We assumed the maximum measured magnitude (${\rm m}_{\rm F606W} = 24.34$ at $\Phi = 0.75$) and an amplitude of variation $\Delta {\rm m}_{\rm F606W} = 3$ between $\Phi = 0.75$ and $\Phi = 0.25$, thus obtaining $\Delta F_{obs} = 2.96 \times 10^{-15}$ erg s^{-1} cm^{-2}. On the other hand, the expected flux variation due to irradiation between $\Phi = 0.75$ and $\Phi = 0.25$ is given by

$$\Delta F_{exp}(i) = \eta \frac{\dot{E}}{a^2} R_{\rm COM}^2 \frac{1}{4\pi d_{\rm PSR}^2} \varepsilon(i)$$

where η is the re-processing efficiency under the assumption of isotropic emission, $R_{\rm COM}$ is the radius of the companion star, which we assumed to be equal to $R_{\rm RL}(i)$, $d_{\rm PSR}$ is the distance of pulsar, adopted to be equal to the GC distance ($d_{\rm PSR} = 7.5$ kpc; Harris 1996; Ferraro et al. 1999) and $\varepsilon(i)$ parametrizes the difference of the re-emitting surface visible to the observer between maximum and minimum[11]. By assuming $\Delta F_{obs} = \Delta F_{exp}(i)$ between $\Phi = 0.75$ and $\Phi = 0.25$, we can derive how η varies as a function of i. The result is shown in Figure 5.

[11] In the following we assume $\varepsilon(i) = (i/180)(1 - R_{\rm COM}/a)$. Note that for $R_{\rm COM} \ll a$ the second term reduces to zero. For the two limit configurations we find that in the case of a face-on system ($i = 0°$), the fraction of the heated surface visible to the observer is constant and hence no flux variation is expected, while in the case of an edge-on system ($i = 90°$) the fraction of the heated surface that is visible to the observer varies between 0.5 (for $\Phi = 0.75$) to 0 (for $\Phi = 0.25$) and hence $\varepsilon = 0.5$.

Obviously, it is important to note that all the calculations have been performed assuming a magnitude modulation of about three magnitudes and hence in case of a larger amplitude of variation the estimated reprocessing would correspond to a lower limit to the true value. As an example, the observed optical modulation can be reproduced considering a system seen at an inclination angle of about 60°, with a very low mass companion ($M_{\rm COM} \sim 0.04 - 0.05 M_{\odot}$) that has filled its RL, and reprocesses the pulsar flux with an efficiency $\eta \gtrsim 1 - 15\%$. Similar results are obtained performing the same calculations in the F390W and F814W bands. It is important to note that, for simplicity, calculations have been performed assuming a RL filled companion (an upper limit to the true companion size). Consequently, in the case of a companion only partially filling its RL the reprocessing efficiency would be larger.

On the other hand, if we use $R_{\rm BB}$ instead of $R_{\rm RL}$ for the stellar radius, the efficiency increases and for several configurations it becomes larger than 100%. In such cases the only possible scenario would be an anisotropic pulsar emission. However, given the presence of eclipses and the observed behavior of other similar objects, $R_{\rm BB}$ is likely too small to provide a good estimate of the companion true physical size. Future studies are needed to better constrain the system parameters.

5. SUMMARY AND CONCLUSION

We obtained a phase-connected radio timing solution of PSR J1518+0204C, including a very precise position and proper motion. The latter is consistent with the known proper motion of two other M5 pulsars, indicating that they are all co-moving because of the cluster motion. We also estimated the time derivative of the orbital period. As common for BW systems, it is larger than the expected contribution due to the emission of gravitational waves. It is much more likely due to tidal dissipation. The precise position of the pulsar was used to identify the companion star (COM-M5C) in the optical bands by using high-resolution WFC3/HST images. COM-M5C turns out to be a very faint but strongly variable star ($\Delta {\rm m}_{\rm F390W} \geq 1.76$, $\Delta {\rm m}_{\rm F606W} \geq 1.33$ and $\Delta {\rm m}_{\rm F390W} \geq 1.28$). Its location in the CMD in a region between the cluster MS and the WD cooling sequence suggests that it is a low-mass star. This is the first companion star to a BW ever detected in a GC. Because of its faintness the star was detected only in 14 out of the 44 available images, whose phases nearly correspond to the pulsar inferior conjunction, while it is below the detection limit at the pulsar superior conjunction. The analysis of the light curve, obtained adopting a simple sinusoidal model, suggests a variation amplitude of about three mags[12], in good agreement

[12]Note that we have considered upper limits estimates when the star was not visible.

with the behavior of other BW companions observed in the Galactic field. Finally, we estimated a lower limit to the reprocessing factor of the pulsar flux ($\eta \gtrsim 1 - 15\%$) by a RL filling companion.

Unfortunately, the star is too faint and located in a too crowded region to allow a spectroscopic follow-up with the available instruments. However, an optimized photometric follow-up aimed to detect the star at the minimum would give the opportunity to better constrain the light curve shape of the companion and hence to better characterize this binary system.

One of the main objectives of this study is to contribute with observational data towards understanding the differences between BW systems in globular clusters and in the Galaxy. This task is important because the formation of these systems is still poorly understood, and it is not known how much it is influenced by the local stellar density. However, given the limited statistics, particularly of systems with optical identifications, a detailed comparison of the two populations is premature at this stage. We refer the reader to a forthcoming paper with the results of a second optical identification of a BW in a globular cluster (M. Cadelano et al. 2014; in preparation).

6. Acknowledgement

This research is part of the project COSMIC-LAB funded by the European Research Council (under contract ERC-2010-AdG-267675). The Arecibo Observatory is operated by SRI International under a cooperative agreement with the National Science Foundation (AST-1100968), and in alliance with Ana G. Méndez- Universidad Metropolitana, and the Universities Space Research Association. Pulsar research at UBC is supported by an NSERC Discovery Grant. J.W.T.H. acknowledges funding from an NWO Vidi fellowship and ERC Starting Grant "DRAGNET" (337062). P.C.C.F. gratefully acknowledges financial support by the European Research Council for the ERC Starting Grant BEACON under contract 279702. C.P. thanks the hospitality from NRAO where most of this work has been developed.

REFERENCES

Alpar, M. A., Cheng, A. F., Ruderman, M. A., & Shaham, J. 1982, Nature, 300, 728

Anderson, S. B., Wolszczan, A., Kulkarni, S. R., & Prince, T. A. 1997, ApJ, 482, 870

Bailyn, C. D. 1992, ApJ, 392, 519

Bailyn, C. D. 1995, ARA&A, 33, 133

Bassa, C. G., Verbunt, F., van Kerkwijk, M. H., & Homer, L. 2003, A&A, 409, L31

Bates, S. D., Bailes, M., Bhat, N. D. R., et al. 2011, MNRAS, 416, 2455

Bellazzini, M., Pasquali, A., Federici, L., Ferraro, F. R., & Pecci, F. F. 1995, ApJ, 439, 687

Bellini, A., & Bedin, L. R. 2009, PASP, 121, 1419

Bellini, A., Anderson, J., & Bedin, L. R. 2011, PASP, 123, 622

Bhattacharya, D., & van den Heuvel, E. P. J. 1991, Phys. Rep., 203, 1

Breton, R. P., van Kerkwijk, M. H., Roberts, M. S. E., et al. 2013, ApJ, 769, 108

Burgay, M., Joshi, B. C., D'Amico, N., et al. 2006, MNRAS, 368, 283

Carretta, E., Bragaglia, A., Gratton, R., & Lucatello, S. 2009, A&A, 505, 139

Chen, H.-L., Chen, X., Tauris, T. M., & Han, Z. 2013, ApJ, 775, 27

Clark, G. W. 1975, ApJ, 199, L143

Cocozza, G., Ferraro, F. R., Possenti, A., et al. 2008, ApJ, 679, L105

Davies, M. B., & Hansen, B. M. S. 1998, MNRAS, 301, 15

Doroshenko, O., Löhmer, O., Kramer, M., et al. 2001, A&A, 379, 579

Dowd, A., Sisk, W., & Hagen, J. 2000, IAU Colloq. 177: Pulsar Astronomy - 2000 and Beyond, 202, 275

Edmonds, P. D., Gilliland, R. L., Heinke, C. O., Grindlay, J. E., & Camilo, F. 2001, ApJ, 557, L57

Edmonds, P. D., Gilliland, R. L., Camilo, F., Heinke, C. O., & Grindlay, J. E. 2002, ApJ, 579, 741

Eggleton, P. P. 1983, ApJ, 268, 368

Ferraro, F. R., Clementini, G., Fusi Pecci, F., & Buonanno, R. 1991, MNRAS, 252, 357

Ferraro, F. R., Fusi Pecci, F., & Buonanno, R. 1992, MNRAS, 256, 376

Ferraro, F. R., Fusi Pecci, F., & Bellazzini, M. 1995, A&A, 294, 80

Ferraro, F. R., Messineo, M., Fusi Pecci, F., et al. 1999, AJ, 118, 1738

Ferraro, F. R., D'Amico, N., Possenti, A., Mignani, R. P., & Paltrinieri, B. 2001a, ApJ, 561, 337

Ferraro, F. R., Possenti, A., D'Amico, N., & Sabbi, E., 2001b, ApJ, 561, L93

Ferraro, F. R., Possenti, A., Sabbi, E., et al. 2003, ApJ, 595, 179

Ferraro, F. R., Possenti, A., Sabbi, E., & D'Amico, N. 2003, ApJ, 596, L211

Ferraro, F. R., Sabbi, E., Gratton, R., et al. 2003c, ApJ, 584, L13

Ferraro, F. R., Beccari, G., Dalessandro, E., et al. 2009, Nature, 462, 1028

Ferraro, F.R. et al., 2012, Nature, 492, 393

Folkner, W. M., Williams, J. G., & Boggs, D. H. 2008, NASA Technical Report, IOM 343R-08-003d

Fregeau, J. M. 2008, ApJ, 673, L25

Freire, P. C. C., Hessels, J. W. T., Nice, D. J., et al. 2005, ApJ, 621, 959

Freire, P. C. C., Wolszczan, A., van den Berg, M., & Hessels, J. W. T. 2008, ApJ, 679, 1433

Fruchter, A. S., Gunn, J. E., Lauer, T. R., & Dressler, A. 1988, Nature, 334, 686

Girardi, L., Bressan, A., Bertelli, G., & Chiosi, C. 2000, A&AS, 141, 371

Goodman, J., & Hut, P. 1989, Nature, 339, 40

Harris, W. E. 1996, AJ, 112, 1487

Hessels, J. W. T., Ransom, S. M., Stairs, I. H., Kaspi, V. M., & Freire, P. C. C. 2007, ApJ, 670, 363

Hills, J. G., & Day, C. A. 1976, Astrophys. Lett., 17, 87

Hut, P., et al. 1992, PASP, 104, 981

Ivanova, N., Heinke, C. O., Rasio, F. A., Belczynski, K., & Fregeau, J. M. 2008, MNRAS, 386, 553

Keith, M. J., Johnston, S., Ray, P. S., et al. 2011, MNRAS, 414, 1292

Keith, M. J., Johnston, S., Bailes, M., et al. 2012, MNRAS, 419, 1752

Lanzoni, B., Dalessandro, E., Ferraro, F. R., et al. 2007, ApJ, 663, 267

Lazaridis, K., Verbiest, J. P. W., Tauris, T. M., et al. 2011, MNRAS, 414, 3134

Lorimer, D. R., & Kramer, M. 2012, Handbook of Pulsar Astronomy, by D. R. Lorimer , M. Kramer, Cambridge, UK: Cambridge University Press, 2012,

Marigo, P., Girardi, L., Bressan, A., et al. 2008, A&A, 482, 883

King, I. 1962, AJ, 67, 471

King, A. R., Davies, M. B., & Beer, M. E. 2003, MNRAS, 345, 678

King, A. R., & Beer, M. E. 2005, Binary Radio Pulsars, 328, 429

Kochanek, C. S. 1996, ApJ, 457, 228

Little, B., & Tremaine, S. 1987, ApJ, 320, 493

Lyne, A. G., Brinklow, A., Middleditch, J., Kulkarni, S. R., & Backer, D. C. 1987, Nature, 328, 399

Lorimer, D. R., Kramer, M., Ellis, R., et al. 2004, Handbook of pulsar astronomy, by D.R. Lorimer and M. Kramer. Cambridge observing handbooks for research astronomers, Vol. 4. Cambridge, UK: Cambridge University Press, 2004,

Meylan, G., & Heggie, D. C. 1997, A&A Rev., 8, 1

Miocchi, P., Lanzoni, B., Ferraro, F. R., et al. 2013, ApJ, 774, 151

Moffat, A. F. J. 1969, A&A, 3, 455

Mucciarelli, A., Salaris, M., Lanzoni, B., et al. 2013, ApJ, 772, L27

Özel, F., Psaltis, D., Narayan, R., & Santos Villarreal, A. 2012, ApJ, 757, 55

Pallanca, C., Dalessandro, E., Ferraro, F. R., et al. 2010, ApJ, 725, 1165

Pallanca, C., Mignani, R. P., Dalessandro, E., et al. 2012, ApJ, 755, 180

Pallanca, C., Dalessandro, E., Ferraro, F. R., Lanzoni, B., & Beccari, G. 2013b, ApJ, 773, 122

Phinney, E. S. 1992, Royal Society of London Philosophical Transactions Series A, 341, 39

Pooley, D., et al. 2003, ApJ, 591, L131

Possenti, A., D'Amico, N., Manchester, R. N., Camilo, F., Lyne, A. G., Sarkissian, J., & Corongiu, A. 2003, ApJ, 599, 475

Pryor, C., & Meylan, G. 1993, Structure and Dynamics of Globular Clusters, 50, 357

Ransom, S. M., Ray, P. S., Camilo, F., et al. 2011, ApJ, 727, L16

Reynolds, M. T., Callanan, P. J., Fruchter, A. S., et al. 2007, MNRAS, 379, 1117

Roberts, M. S. E. 2013, IAU Symposium, 291, 127

Romani, R. W. 2012, ApJ, 754, L25

Sigurdsson, S., Richer, H. B., Hansen, B. M., Stairs, I. H., & Thorsett, S. E. 2003, Science, 301, 193

Stappers, B. W., Bailes, M., Lyne, A. G., et al. 1996a, ApJ, 465, L119

Stappers, B. W., Bessell, M. S., & Bailes, M. 1996b, ApJ, 473, L119

Stappers, B. W., van Kerkwijk, M. H., Lane, B., & Kulkarni, S. R. 1999, ApJ, 510, L45

Stappers, B. W., van Kerkwijk, M., & Bell, J. F. 2000, IAU Colloq. 177: Pulsar Astronomy - 2000 and Beyond, 202, 627

Stappers, B. W., van Kerkwijk, M. H., Bell, J. F., & Kulkarni, S. R. 2001, ApJ, 548, L183

Stetson, P. B. 1987, PASP, 99, 191

Stetson, P. B. 1994, PASP, 106, 250

Taylor, J. H. 1992, Royal Society of London Philosophical Transactions Series A, 341, 117

van Kerkwijk, M. H., Breton, R. P., & Kulkarni, S. R. 2011, ApJ, 728, 95

Verbunt, F., Bunk, W. H., Ritter, H., & Pfeffermann, E. 1997, A&A, 327, 602

Verbunt, F., & Freire, P. C. C. 2014, A&A, 561, A11

This preprint was prepared with the AAS LaTeX macros v5.2.

Table 1. Parameters for PSR J1518+0204C

Parameter	Value
Right Ascension, α (J2000)	$15^{\rm h}\ 18^{\rm m}\ 32\overset{\rm s}{.}788893(21)$
Declination, δ (J2000)	$02^\circ\ 04'\ 47\overset{''}{.}8153(8)$
Proper motion in α, μ_α(mas yr^{-1})	4.67(14)
Proper motion in δ, μ_δ(mas yr^{-1})	$-8.24(36)$
Dispersion Measure (pc cm^{-3})	29.3146(6)
Span of Timing Data (MJD)	52484 - 55815
Number of TOAs	1398
Weighted RMS Timing Residual (μs) ..	12
Spin Parameters	
Pulsar Frequency, ν (Hz)	402.58822840843(9)
Frequency Derivative, $\dot{\nu}$ (Hz/s)	$-4.2252(2)\times10^{-15}$
Frequency 2nd Derivative, $\ddot{\nu}$ (Hz/s^{-2}) ..	$-1.45(16)\times10^{-26}$
P Epoch (MJD)	52850.0000
Orbital Parameters	
Orbital Period, P_{orb} (days)	0.08682882865(3)
Projected Semi-Major Axis, $a \sin i$ (lt-s)	0.05732042(57)
Eccentricity, e	0.0000000000
Epoch of Ascending Node, T_{asc} (MJD) .	52850.00434606(17)
Orbital Period Derivative, $\dot{P}_{orb}$ (s/s) ...	$-0.914(23)\times10^{-12}$
Derived Parameters	
Pulsar Period, P (ms)	2.48392757024730(22)
Period Derivative, $\dot{P}$ (s/s)	$2.6055(12)\times10^{-20}$
Mass Function, f_1 ($M_\odot$)	$2.68177(14)\times10^{-5}$
Minimum Companion Mass, m_2 ($M_\odot$) .	≥ 0.038

Note. — Numbers in parentheses represent the formal errors in the least significant digits as determined by a bootstrap analysis of the data with 4096 iterations. The pulsar is assumed to have a mass of $1.4\,M_\odot$.

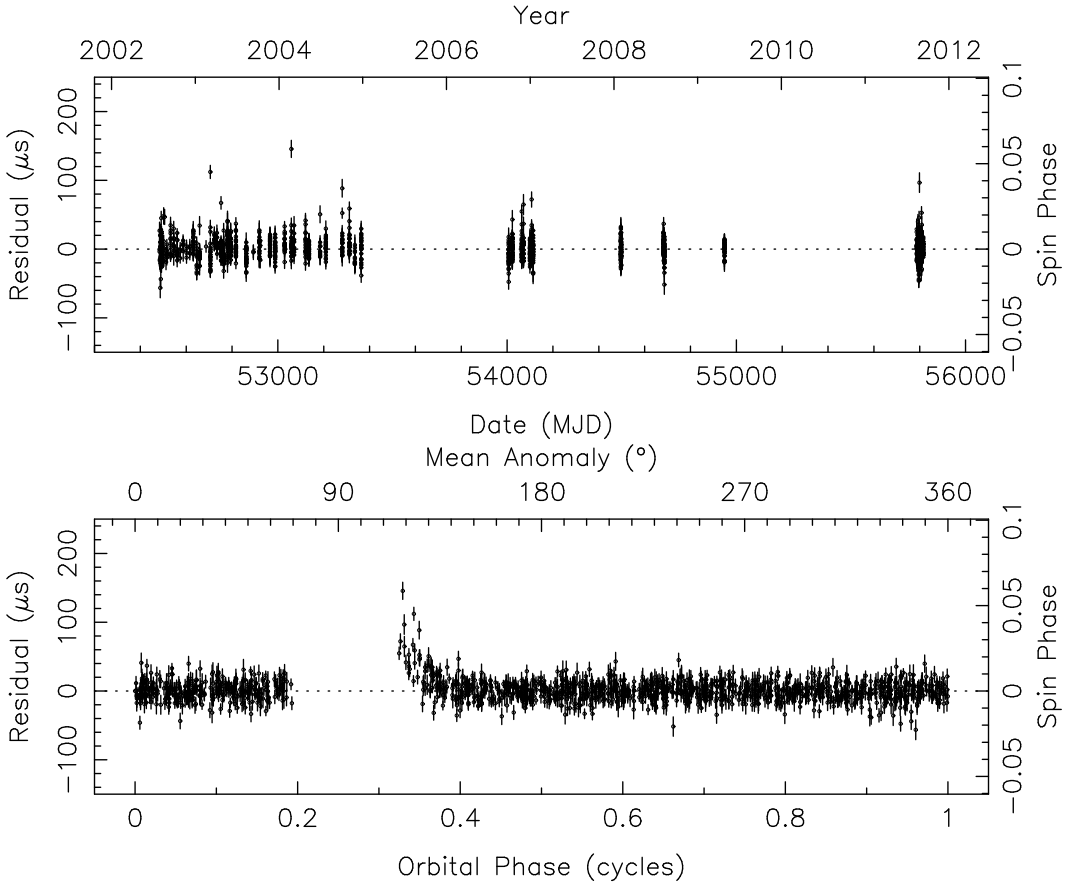

Fig. 1.— Timing residuals for PSR J1518+0204C. The top panel shows the post-fit timing residuals of the timing solution described in Table 1 as a function of date (in MJD). The weighted RMS of the residuals is 12.3 μs based on1398 arrival times. The bottom panel shows post-fit residuals as a function of the orbital phase (mean anomaly), where the radio eclipse is obvious near orbital phase 0.25 (pulsar superior conjunction). Arrival times between the orbital phases of 0.2 and 0.38 are not among the 1398 used in the timing fit, but are displayed here to illustrate the extra dispersive delay near superior conjunction, which is due to plasma emanating from the companion star.

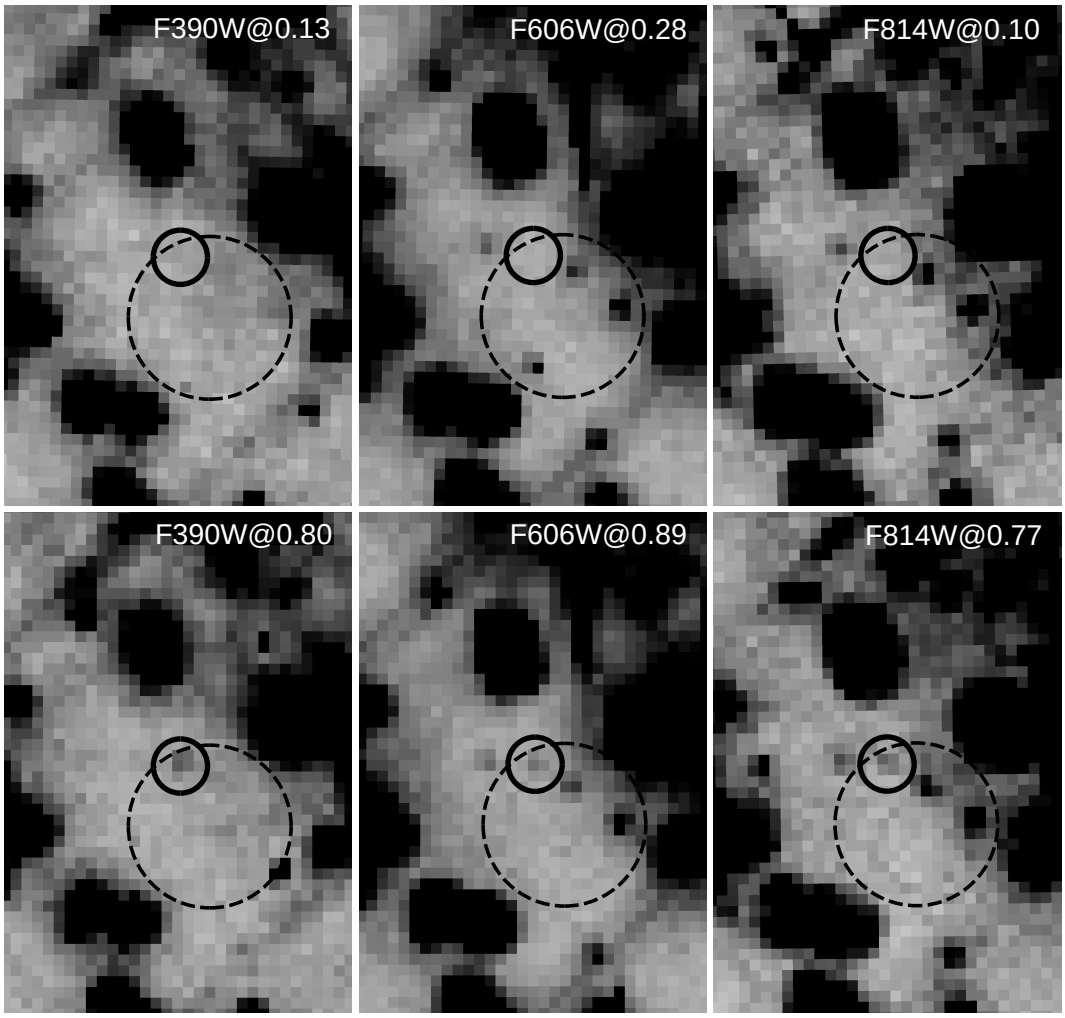

Fig. 2.— HST images of the $1.3'' \times 1.8''$ region around the nominal position of PSR J1518+0204C. The filters and orbital phases are labelled in each panel. The dashed circle of radius $0.3''$ (of the order of the optical astrometric uncertainty) is centered on the radio-band pulsar position. The solid circles indicate the identified companion star. It is clearly visible in the lower panels (at about the pulsar inferior conjunction), while it disappears in the upper panels (at about the pulsar superior conjunction).

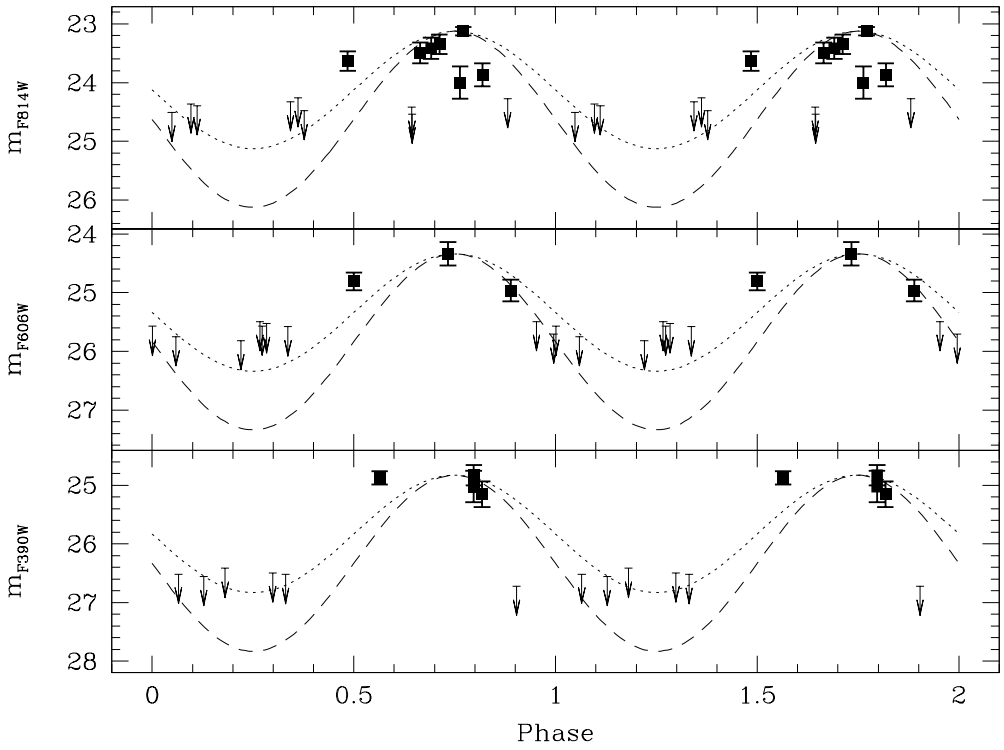

Fig. 3.— The observed light curve of the companion to PSR J1518+0204C folded with radio timing orbital parameters. The arrows are the estimated upper-limits to the magnitude for the images where the star is below the detection threshold. The dotted and dashed lines are sinusoidal first-guess models of the light curve, with amplitudes of two and three magnitudes, respectively. Note that the latter model is in agreement with most of the upper limits. However, the light curve does not look as a perfect sinusoid, in agreement with the models of Breton et al. (2013) calculated for similar objects.

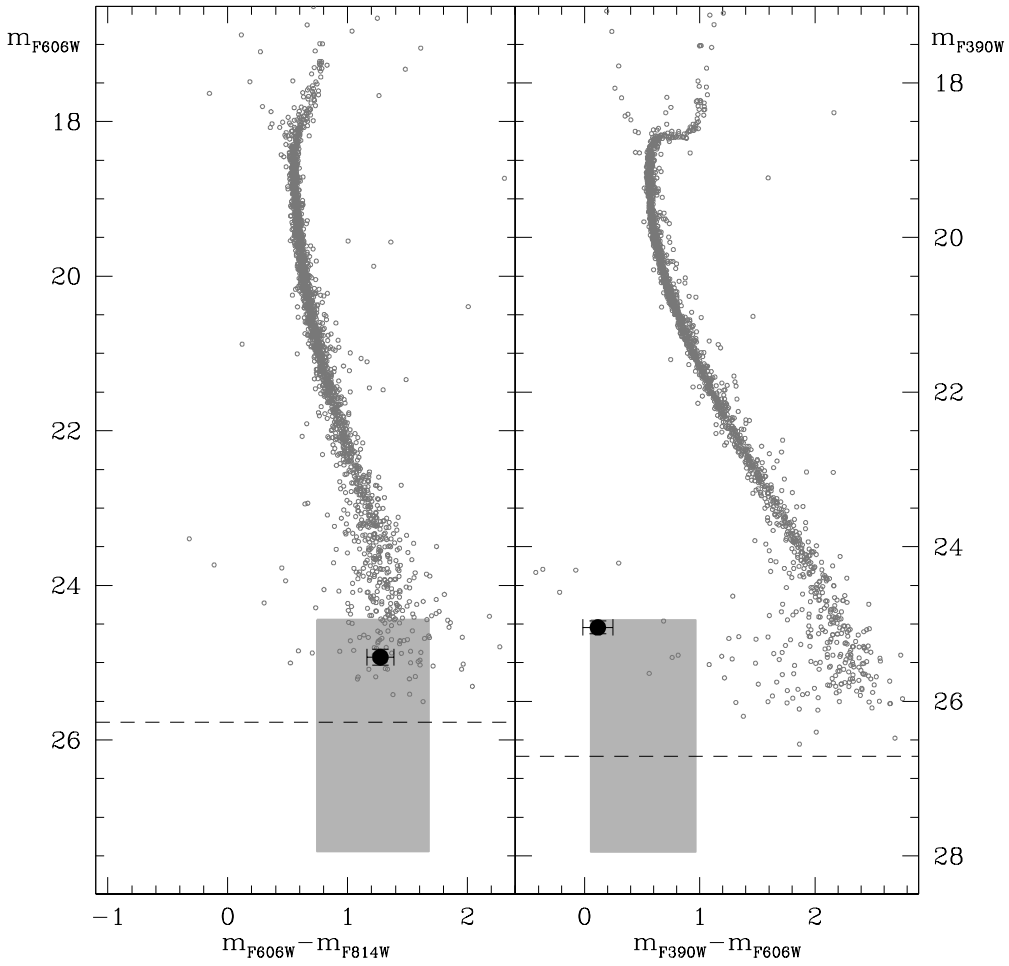

Fig. 4.— Optical CMDs defined by all stars detected within 10″ from the pulsar nominal position (gray circles). The dashed lines correspond to the detection limits in the F606W and F390W bands (left and right panel, respectively). In each panel the black dot marks the position of COM-M5C as obtained from the average of the measured values. However, such a location is biased by the under-sampling of the light curve. Hence, by taking into account the magnitude modulation we report the possible location of the companion star. In particular, the magnitude ranges between the measured maximum and a minimum assumed to be three magnitudes fainter, while the color has been calculated as the color at maximum, with an uncertainty estimated to be of the order of the standard deviation shown by objects with similar magnitudes. Therefore, COM-M5C turns out to be located between the MS and the WD loci.

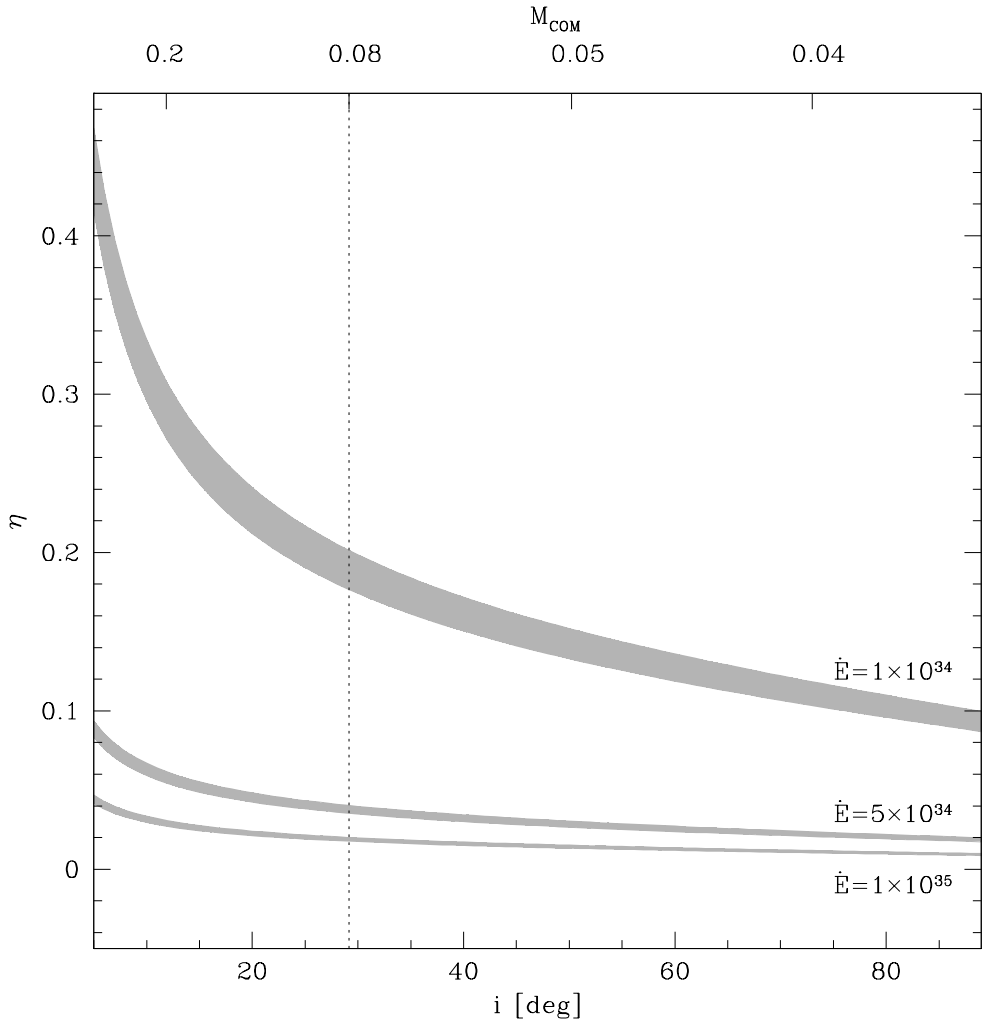

Fig. 5.— Lower limit to the reprocessing efficiency for isotropic emission (η) calculated as a function of the inclination angle (i) and assuming a magnitude modulation (Δmag = 3 mags). The three gray strips correspond to different values of $\dot{E}$: 1.0×10^{34}, 5.0×10^{34} and 1.0×10^{35} erg/s, respectively from top to bottom. The thickness of each strip corresponds to a pulsar mass ranging from $1.24 M_{\odot}$ to $2.5 M_{\odot}$. On the top axis, the companion masses in units of $M_{\odot}$ (calculated by assuming a $M_{\rm PSR} = 1.4 M_{\odot}$) are reported. The dotted line marks the physical limit ($M \gtrsim 0.08 M_{\odot}$) for core hydrogen burning stars.